UCSB ChE's 5th Clorox-Amgen Grad Student Symposium

Oral Presentation Abstracts

Session I:
Biophysics and Bioengineering

Filming hydration and conformational dynamics to understand transmembrane protein function

Sunyia Hussain[(a)], Maia Kinnebrew[(b)], Aye Aye[(c)], and Songi Han[(a,c)]

(a) Department of Chemical Engineering, University of California, Santa Barbara
(b) Department of Biology, University of California, Santa Barbara
(c) Department of Chemistry and Biochemistry, University of California, Santa Barbara

Transmembrane proteins are the gatekeepers of the cell, operating from their key position embedded in the cell membrane. They fulfill diverse and important functions, acting as sensors of the outside environment or transporters of molecules across the hydrophobic membrane barrier. The range of interactions occurring within the cell membrane between proteins, lipids, and the surrounding aqueous environment presents a complex system, distinguished from water-soluble biomolecules. Here, we present work towards understanding the role of the membrane assembly in tuning the function of seven-helical transmembrane (7TM) proteins—a broad class of biomolecules including many physiologically vital receptors. We focus on the light activation and functional properties of a prototypical example, the Proteorhodopsin (PR) proton pump from marine bacteria. A combination of spectroscopic techniques uncovers unique information about the dynamics that govern PR function. We observe how the protein and surrounding hydration water rearrange upon activation, and further how these dynamics are affected by the surrounding environment, encompassing both protein-protein and protein-lipid interactions. This is made possible by the application of the powerful residue-specific magnetic resonance methods of electron paramagnetic resonance (EPR), which measures protein segment mobility, and Overhauser dynamic nuclear polarization (ODNP), as recently-developed in the Han group for probing local water diffusivity within 10 Å of a nitroxide spin-label. With these techniques together with optical absorption spectroscopy, we gain evidence that water dynamics at the membrane protein surface is affected by the surfactant environment and furthermore, it modulates the timescale of conformational motion and therefore the efficiency of protein function. Our work also reveals that the association of PR with other PR molecules within the membrane, or oligomerization, has similar functional consequences in addition to effects on the protonation properties of key residues for ion transport.

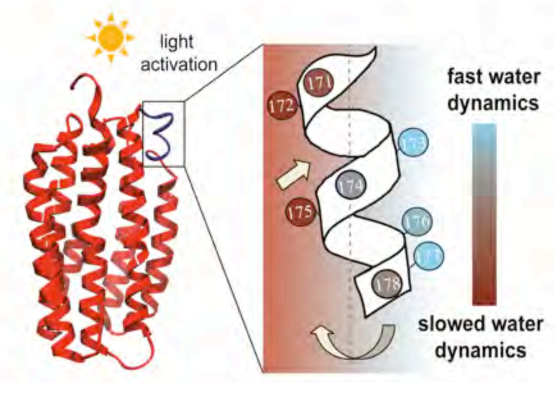

Figure 1: Changes in the hydration landscape of Proteorhodopsin's E-F loop upon light activation.

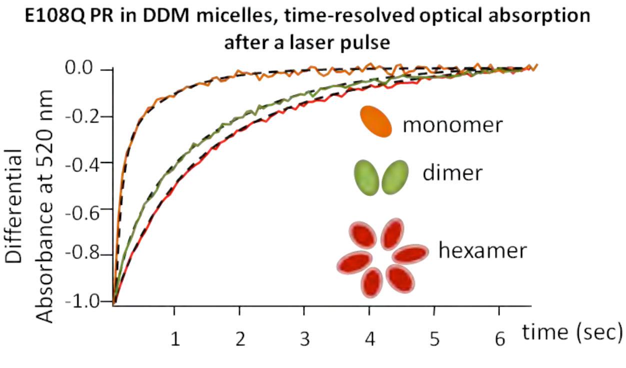

Figure 2: Kinetics of PR conformational change for different oligomeric forms constituted in DDM detergent micelles

Serum Antibody Profiling of Celiac Disease Using Bacterial Display for *in vitro* Diagnostics

Bradley N. Spatola and Patrick S. Daugherty

Chemical Engineering Department, University of California at Santa Barbara, Santa Barbara, CA 93106

Celiac disease (CD) is an autoimmune disease of the small intestine affecting genetically susceptible individuals following the ingestion of gluten, a protein found in wheat. Although the combination of a serological test with a small intestinal biopsy is a highly effective method for CD diagnosis, there are still critical questions that need to be addressed: the ability to confidently diagnose a patient based on serology alone, identifying additional trigger antigens involved in disease pathogenesis and monitoring patient recovery while on a gluten-free diet. A new serum antibody profiling strategy has been optimized to selectively detect antibodies from CD patients but not detect antibodies from a control patient set. Quantitative specificity-based display library screening was performed by multi-color fluorescent activated cell sorting (FACS) as shown in Figure 1. In order to determine which mimotopes, or peptides that mimic antigenic determinants, had the highest predictive value for CD, the cross-reactivity of these mimotopes was tested on an individual patient basis with the patients from the ligand discovery phase. Multiple new patient cohorts, not involved in the discovery phase, acquired from CD clinicians in Finland and the United States were used to train a predictive classification algorithm that correctly classifies patients as either CD or healthy by combining the reactivity of antibodies against six mimotopes isolated from the display library. Validation of the algorithm with new patients yields a classifier accuracy of 80%. Although less than the current highly optimized serological tests for CD that achieve greater than 90% specificity and sensitivity, the high classifier accuracy indicates that this new serum profiling methodology is a general, unbiased approach to identify diagnostically relevant antibody-peptide interactions. This specificity-based display library screening technique will be applied to CD patients who respond to a gluten-free diet in order to discover an antibody signature indicative of small intestinal recovery. With further optimization, this global antibody profiling approach has applications to other autoimmune diseases and possibly cancer for noninvasive and low cost diagnostic purposes.

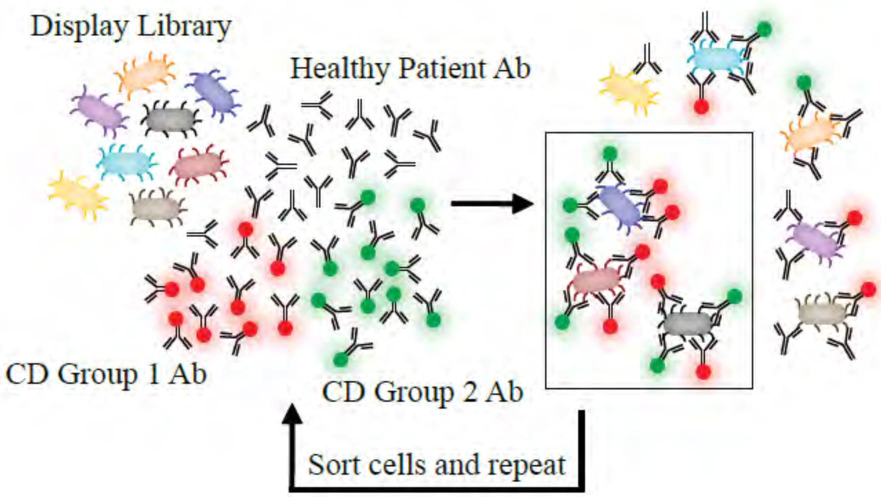

Figure 1: Specificity-based cell display library screening methodology.

Photo-activated drug release from temperature sensitive liposomes using hollow gold nanoshells

Natalie Forbes(a) and Joseph A Zasadzinski(b)

(a) Department of Chemical Engineering, University of California, Santa Barbara
(b) Department of Chemical Engineering and Materials Science, Univeristy of Minnesota

A drug delivery system with rapid contents release under continuous-wave near-infrared (NIR) light will enable precise spatial and temporal control of drug release. The drug is encapsulated within temperature sensitive liposomes, and rapid drug release is triggered by the photothermal heating of hollow gold nanoshells coupled to the liposome surface. The membrane lipid composition can be tuned to achieve near-complete triggered release at temperatures between 39-45°C. Under irradiation at physiological temperature, the nanoshells locally heat the liposome membrane to the phase transition temperature and thereby increase membrane permeability. A fluorescent dye was encapsulated as a model agent to study release kinetics and to empirically estimate the heat generated by the nanoshells under irradiation. The anticancer agent doxorubicin was then encapsulated within the liposomes and delivered to prostate cancer cells (PPC-1) to investigate the impact on cell viability.

Articular Joint lubrication and the wear mechanism under mild conditions

Dong Woog Lee(a), Xavier Banquy(a), and Jacob Israelachvili(a,b)

(a) Department of Chemical Engineering, University of California, Santa Barbara
(b) Materials Department, University of California, Santa Barbara

Cartilage is the primary tissue in articular joints, which actually is being sheared during all kinds of articular motion. In other words, if not perfectly protected, cartilage is highly susceptible to frictional damage due to the various kinds of shearing conditions it experiences. Extreme conditions such as high load, fast shearing speed are critical for cartilage integrity, however, it is surprising that many people suffer from pain when they get up from the sleep, sit or stand still for a long time which is known to be 'mild' conditions for cartilage.

In this work, we investigated the frictional behavior of cartilage using surface force apparatus (SFA) in mild conditions at slow driving speed (0.3~60 μm/s) and low pressure (0.1~2 atm). Specific enzymes (Hyaluronidase, Type II Collagenase and Chondroitinase ABC) are treated for further investigation of the role of each component. Cartilage surface was also imaged using light interferometer to quantify the roughness changes after digestion and shearing.

We observed stick-slip friction in articular cartilage for the first time, in a certain range of loads and speeds. We introduced 'Dynamic (friction) phase diagram' to visualize load and speed regimes of stick-slip friction. Significant increase in friction force was observed after digestion (~ 2 times for Hyaluronidase, ~5 times for Collagenase and ~10 times for Chondroitinase ABC) with apparent roughening (Hyaluronidase and Chondroitinase ABC) or smoothening (Collagenase) of cartilage surface. Moreover, we found that there is minor contribution of topography (roughness) to frictional behavior of articular cartilage, which is contradictory to general knowledge of tribology.

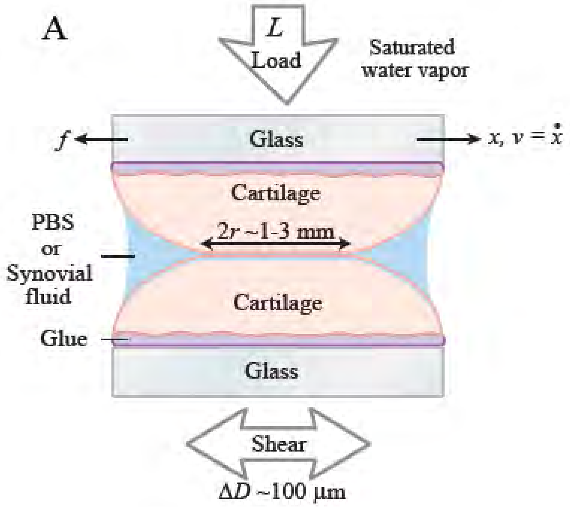

Figure 1: Schematic of the experimental set up. A pair of dissected cartilages were glued on to two flat discs and sheared under constant velocity *v*, under the load of *L*. Peak to Peak shearing distance Δ*D* was around ~100 μm.

Session II:
Complex Fluids, Colloids and Interfaces

On the Surface Shear Viscosity of Soluble Surfactants

Zachary A. Zell, L. Gary Leal and Todd M. Squires

Department of Chemical Engineering, University of California, Santa Barbara

The stability and flow behavior of multiphase materials like foams and emulsions are closely linked to their interfacial properties, which can be greatly affected by the presence of surfactants. One such important property is the surface shear viscosity, as it is generally thought to enhance stability via reduced film drainage. The understanding of surfactant effects on surface shear viscosity is thus crucial to the study of such materials. However, for a common anionic surfactant used to make foams, sodium dodecyl sulfate(SDS), the reported values of measured surface viscosities vary by several orders of magnitude (0.01-100μNás/m). In this study, we use ferromagnetic microdisks deposited at the SDS solution - air surface, as active, microrheological probes of the interface. Our oscillatory shear measurements reveal that the values of surface shear viscosity are on the order of 0.01μNás/m or lower, at which point the probe becomes Boussinesq limited. We therefore question the interpretation of previous measurements, and thus of the reported values of the surface viscosity of SDS solutions. Instead, we suggest that the non-viscometric flow (including compression and dilation) gives rise to enhanced drag forces that do not reflect shear viscosity. Rather, we propose that the enhanced drag coefficients in the literature are likely due to Marangoni forces and not the surface shear viscosity. Our results suggest that the generally-believed correlation between the surface shear viscosity of surfactants, and the stability of foams and emulsions made using them, is not correct, but instead reflects other physico-chemical processes.

Interfacial microrheology of model lung surfactant monolayers

KyuHan Kim, Siyoung Q, Choi, Joseph A. Zasadzinski and Todd M. Squires

Chemical engineering, University of California, Santa Barbara

Cholesterol plays a significant role in biological interfaces and membranes, such as cell membranes and lung surfactant monolayers. We are particularly interested in lung surfactants (LS) monolayers, where the role of cholesterol remains unclear. Furthermore, even though a small mole fraction of cholesterol (5-10%) has been reported in extracts of mammalian LS, there is still a question whether cholesterol originates from the LS or from cell debris. We have interested the mechanical properties of LS monolayers, which may keep the LS deep inside the lungs and make respreading of LS easily during respiration. Here, with varying cholesterol fractions from 0 to 5.5 mol% in DPPC monolayers where the morphology and mechanical properties of the films change dramatically, we systematically measure the mechanical properties of DPPC/cholesterol mixtures as a simple model of LS, using micro-fabricated ferromagnetic micro-buttons as new rheological probes [1, 2]. In addition, using atomic force microscopy (AFM) and fluorescence microscope, we show the change in equilibrium structures with varying cholesterol amounts to understand the dynamic processes. As a result, we show that cholesterol segregates into line-active nanodomains at domain boundaries, and increasing the cholesterol content to 5 mol% entangles the grain boundaries and induces an elastic response, causing the monolayer to react as a soft solid, while the viscosity remains low. This elasticity likely stabilizes the monolayer, promoting low surface tension on compression.

References:

[1] Choi, S. Q.; Steltenkamp, S.; Zasadzinski, J. A.;Squires, T. M. *nature comm.* **2011**, *2* 312.
[2]Kim, K.; Choi, S. Q S.; Zasadzinski, J. A.;Squires, T. M *Soft matter.* **2011**, *7*, 7782.

Microstructural Transformations in Concentrated, Charged Vesicle Suspensions

Mansi Seth [a], Arun Ramachandran [b], L. Gary Leal [a]

(a) Department of Chemical Engineering, University of California, Santa Barbara
(b) Department of Chemical Engineering and Applied Chemistry, University of Toronto

It is observed that charged unilamellar vesicles in a suspension can spontaneously deflate and subsequently transition to form bilamellar vesicles, even in the absence of externally applied triggers such as salt or temperature gradients. We show that the driving force for this deflation-induced transition is the repulsive electrostatic pressure between charged vesicles in concentrated suspensions. We use cryoTEM imaging to quantitatively follow the time-evolution of cationic DEEDMAC vesicle suspensions at different surfactant and salt concentrations and elucidate the role of these two parameters on the initiation of spontaneous vesicle deflation. A simple model based on the Gouy-Chapman theory of electrostatics in solutions is developed to estimate the extent of deflation of unilamellar vesicles caused by electrostatic interactions with neighboring vesicles. It is determined that above a critical effective volume fraction that depends upon vesicle size and both surfactant and salt concentration, charged vesicles in a suspension can experience '*crowding*' due to overlap of their electrical double layers, which can result in deflation and subsequent microstructural transformations to reduce the effective volume fraction of the suspension, given that the vesicles are in the fluid sate. When the vesicles are in the gel state at room temperature, similar conditions lead to the formation of 'jammed' suspensions that behave like viscoelastic gels. This is reminiscent of colloidal suspensions of charged hard-spheres that form ordered phases above a critical volume fraction [1].

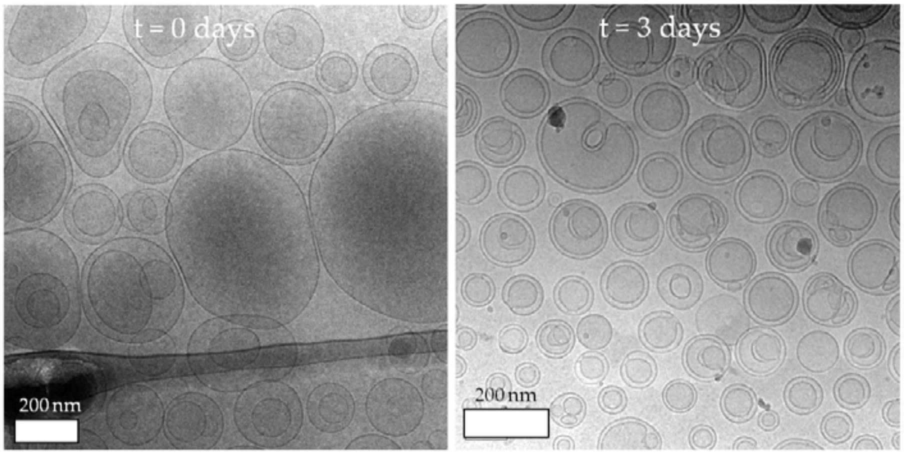

Figure 1: CryoTEM images of a DEEDMAC suspension in 4.5 mM CaCl2. 1a: After preparation (t = 0), 100 -200 nm sized unilamellar vesicles interacting with neighboring vesicles. 1b: After 3 days, the relative fraction of vesicles smaller than 100 nm in diameter with 2 bilayers, i.e. doublets is found to increase.

[1] Larson, RG. The Structure and Rheology of Complex Fluids, **1999**, Oxford University Press: New York

Development of a general interaction potential for hydrophobic and hydrophilic interactions

Stephen Donaldson, Markus Valtiner, Bradley Chmelka, and Jacob Israelachvili

University of California Santa Barbara, Department of Chemical Engineering

Hydrophobic interactions, driven by the inability of water molecules to hydrogen bond in the vicinity of hydrophobic molecules and surfaces resulting in strong, long range attractive interactions between hydrophobic moieties, are ubiquitous in the self-assembly of complex structures and many physical and biological processes, such as protein folding, bio-membrane adhesion and fusion, and drug-delivery vehicles. Hydrophilic interactions are similarly ubiquitous. Hydrophilic molecules or surfaces have several layers of strongly bound water molecules, which become increasingly more difficult to dehydrate as the water gap decreases, resulting in a strongly repulsive hydration interaction. A quantitative, theoretical description of both interactions has remained elusive, especially in cases where both interactions determine the final self assembled state, such as heterogeneous surfaces common in protein folding, bio-membranes and detergent action. Recent surface forces apparatus (SFA) measurements allowed us to obtain a hydrophobic interaction potential, and the model quantitatively captures the long range forces, short range forces, breakthrough point, and final hydrophobic adhesion as two bilayers approach, spread (thin), rupture, hemi-fuse, and are then separated from adhesive contact. These results indicate that the hydrophobic interaction depends on the interfacial tension ($\gamma_\mathrm{i} \sim 50$ mJ/m^2) and excess exposed hydrophobic area (which increases as the bilayer is stressed), with an exponential decay with a decay length of 1 nm.

More recent analysis has shown that our model can also apply to the case of excess *hydrophilic* area, and quantitative agreement with previous surface forces experiments is obtained, with an identical decay length and pre-exponential factor. A new picture is emerging, which suggests both water-based interactions can be described by a single unifying equation, and perhaps indicates a similar mechanism for both interactions: for example, increased water density (and/or hydrogen bonding order parameter) near hydrophilic surfaces, and depleted water density (and a corresponding decrease of the order parameter) near hydrophobic surfaces.

Session III:
Modeling, Simulations and Control

A Systematic Coarse-graining of Molecular Dynamics Simulations: Thermodynamic and Transport Properties

Chia-Chun Fu, Pandurang M. Kulkarni, M. Scott Shell and L. Gary Leal

Department of Chemical Engineering, University of California, Santa Barbara

Coarse-graining techniques have recently attracted great interest for providing descriptions at a mesoscopic level of resolution that preserve fluid thermodynamic and transport behaviors with a reduced number of degrees of freedom (DOFs) and hence less computational effort. One fundamental question arises: how well and to what extent can a “bottom-up” developed mesoscale model recover the physical properties of a molecular scale system? To answer this question, we explore systematically the properties of a coarse-grained (CG) model that is developed to represent an intermediate mesoscale model between the atomistic and continuum scales [1,2]. We first use the iterative Boltzmann inversion (IBI) to determine a CG potential for a $(1-\phi)N$ mesoscale particle system, where ϕ is the degree of coarse-graining, so as to reproduce the radial distribution function (RDF) of an N atomic particle Lennard-Jones (LJ) system. Even though the uniqueness theorem guarantees a one to one relationship between the RDF and an effective pairwise potential, we find that RDFs are insensitive to the long-range part of the IBI-determined potentials, which provides some significant flexibility in further matching other properties. We then propose a reformulation of IBI as a robust minimization procedure that enables simultaneous matching of the RDF and the fluid pressure. This new method mainly changes the attractive tail region of the CG potentials, and it improves the isothermal compressibility relative to pure IBI. We also find that there are optimal interaction cutoff lengths for the CG system, as a function of ϕ, that are required to attain an adequate potential while maintaining computational speedup. Unlike the RDF and the virial pressure, dynamical properties such as the self diffusion coefficient and viscosity cannot be matched directly during coarse-graining by modifying the pair interaction. A simple but approximate approach is to introduce a friction coefficient, γ, and random forces for the remaining degrees of freedom, in which case γ becomes an additional parameter in the coarse-grained model that can be tuned. We consider the Galilean-invariant dissipative particle dynamics thermostat and show that a value of γ for each degree of coarse-graining ϕ can be found for which both viscosity and diffusion match the reference LJ liquid. Importantly, we show that Stokes-Einstein behavior persists for these coarse models and offers a useful perspective for interpreting the dynamics of mesoscale CG models.

References:
[1] Fu, C.; Kulkarni, P.; Shell, M. S.; Leal, L. G. *J. Chem. Phys.* **2012**, Submitted.
[2] Fu, C.; Kulkarni, P.; Shell, M. S.; Leal, L. G. *J. Chem. Phys.* **2012**, Submitted.

Using Explicitly Treated Pair-wise Simulations, Mean-field Models, and Scaling Relations of Electric Double Layers to Asses the Consequences of the Guoy-Chapman Assumptions

Brian Giera(a,b), Ed Kober(b), Scott Shell(a), and Todd Squires(a)

(a) Department of Chemical Engineering, University of California, Santa Barbara
(b) Institute for Multiscale Materials Studies, Los Alamos National Laboratory, Los Alamos, New Mexico

Nanoscale ionic clouds called electric double layers (EDLs) form at all interfaces between electrolytes or ionic liquids and a charged surface such as an electrode, colloid, protein, or cell membrane. The EDL plays a central role in colloidal and polyelectrolyte science, nanofluidics, and in electric double-layer capacitors (EDLCs, or supercapacitors) that store energy chemically across the EDL. A detailed understanding of EDL structure is important in determining differential capacitiance, electrokinetic flow, and rational design of EDLCs. The standard starting point for modelling fully charged EDLs is the Guoy-Chapman approach, which assumes an EDL comprised of point-sized ions, in an implicit solvent with uniform properties, and that the ions only interact electrostatically with a charged flat electrode. We compare GC against 100+ simulations that span a wide range of dimensionless paramater space to evaluate when it is acceptable to make GC assumptions, when they breakdown, and explain the mechanisms when they fail. We find that all mean-field and atomistic models of the EDL agree with GC in a common region of parameter space that is physically described by dilute ion concentrations far weakly charged electrodes.

Gibbs Ensemble Calculations of Phase Coexistence in Supramolecular Assembly of Block Copolymers

Zoltan Mester(a), Nathaniel Lynd(b), Kris Delaney(b), and Glenn Fredrickson 4(a,b)

(a) Department of Chemical Engineering, University of California, Santa Barbara
(b) Materials Research Laboratory, University of California, Santa Barbara

We propose a new self-consistent field theory method for calculating phase behavior in reversibly bonded supramolecular polymer melts. Previous studies formulated models for supramolecular assembly in the grand canonical ensemble to make use of the constraints imposed on the chemical potentials of the products from chemical equilibrium. Instead, we formulate the model in the canonical ensemble by including a term in the Hamiltonian that accounts for the reaction favorability/penalty. The chemical equilibrium statement is obtained by optimizing the Hamiltonian with the amount of reacted polymer. The canonical partition function can be easily adapted to the Gibbs ensemble whereby phase boundaries between coexisting phases can be conveniently simulated. As an illustration of our method, we examine a blend of AB diblock and B homopolymer with the ability to reversibly bond to form ABB diblock. In the limits of infinite reaction favorability and penalty, the system approaches cases of an ABB diblock-B homopolymer blend when the AB diblock is the limiting reactant and an AB diblock-B homopolymer blend, respectively. The interplay between reactant ratios (stoichiometry) and reaction favorability/penalty is explored for intermediate values of reactivity. There is an additional effect on phase behavior of having longer diblocks when reaction is favorable. It is demonstrated that most of the phases found in regular diblock blend are recovered by varying the reaction energy and composition.

Development and Implementation of the Health Monitoring System for the Artificial Pancreas

Rebecca A. Harvey(a,b), Eyal Dassau (a,b), Howard Zisser (a,b) , and Francis J. Doyle III(a,b)

(a) Department of Chemical Engineering, University of California, Santa Barbara
(b) Sansum Diabetes Research Institute, Santa Barbara

Type 1 diabetes mellitus (T1DM) is a metabolic disease in which blood glucose (BG) cannot be adequately regulated due to the destruction of insulin-producing pancreatic beta cells. People with T1DM must monitor BG and inject insulin several times a day in order to thrive and avoid complications of hypoglycemia (low BG, <70 mg/dL) and hyperglycemia (high BG, >180 mg/dL). The ultimate goal of the artificial pancreas device system (APDS), a combination of continuous glucose monitor (CGMs), insulin delivery device, a control system that executes insulin delivery, and a safety system is controlling BG automatically . The Health Monitoring System (HMS) is a safety system parallel to the control algorithm for the APDS that automatically checks that state of the device and user and relays information to the user and physician[1,2].

HMS will include several safety modules, including hypoglycemia, hyperglycemia, and missed meal detection; pump and sensor error detection; and communication monitoring. The Low Glucose Predictor (LGP) was designed as the primary module of the HMS that pre-processes data and predicts hypoglycemia. These data are sent to the HMS to issue local audible and visual alerts and are automatically transmitted as short and multimedia messages (SMS and MMS)[3]. These messages are sent to the physician in charge or other primary contact with a plot of the current trend and short-term prediction. The alarms are acted upon by administration of 16g of rescue carbohydrates.

The LGP was designed using retrospective CGM data and evaluated *in silico* using the FDA-accepted UVA/Padova metabolic simulator[4]. The HMS with LGP was validated in a series of twelve clinical trials in conjunction with a Zone-Model Predictive Control controller[5]. The trials were each approximately 24 hours, with challenges including two unannounced meals and an exercise session. A total of 46 HMS alarms were issued with 4 ± 2 alarms per subject at an average CGM value of 82 ± 11 mg/dL. Within 30 minutes on average, the CGM value had increased by 10 mg/dL, indicating a return to the target glucose range and a recovery from hypoglycemia. Overall, only 2% of time was spent below 70 mg/dL. The HMS was shown in these trials to effectively detect adverse events that were potentially unavoidable by controller action.

The HMS has been designed as a safety system in parallel to APDS that alerts and mitigates adverse events. This design ensures user safety and adds robustness to the overall system without interfering with the primary controller. The ability of the HMS to be an effective alert system that provides a safety layer to the APDS controller has been clearly demonstrated in clinic, detecting events that were unavoidable even with appropriate controller action. With use of the HMS, adverse events that are not handled by the controller are readily detected and mitigated.

References:
[1] Harvey, R. A.; Dassau, E.; Zisser, H.; Seborg , D. E.; Jovanovič, L.; Doyle III, F. J. *J Diabetes Sci Technol (Under Review)* **2012**.
[2] Doyle III, F. J.; Dassau, E.; Zisser, H.; Harvey, R. A., *Health Monitoring System*, US Patent Application Number 13/166,806, Submitted 2011.
[3] Dassau, E.; Jovanovič, L.; Doyle III, F. J.; Zisser, H. *J Diabetes Sci Technol* **2009**, *3*, 1501.
[4] Kovatchev, B. P.; Breton, C.; Dalla Man, C.; Cobelli, C. *J Diabetes Sci Technol* **2009**, *3*, 44.
[5] Grosman, B.; Dassau, E.; Zisser, H. C.; Jovanovič, L.; Doyle III, F. J. *J Diabetes Sci Technol* **2010**, *4*, 961.

Session IV:
Materials, Energy and Catalysis

Spatially-resolved spectral mapping of phase mixing and charge transfer excitons in bulk heterojunction solar cell films

Isaac Riisness, Chris Carach, and Mike Gordon

Department of Chemical Engineering, University of California-Santa Barbara, Santa Barbara

Donor-acceptor phase mixing and charge transfer excitons (CTXs) in bulk heterojunction solar cell films were imaged using a custom-built confocal photoluminescence (PL) and Raman microscope. Spatially-resolved spectral analysis of PL was used to map fullerene diffusion and agglomeration during thermal annealing as well as detect local changes in interfacial contact between donor and acceptor domains. CTX emission was most intense at the periphery of micron-sized fullerene agglomerates, which correlates with fullerene depletion in the surrounding film. Raman scattering indicates that the polymer phase is essentially immobile during the annealing process and that fullerene agglomerates reside on top of a polymer-rich underlayer.

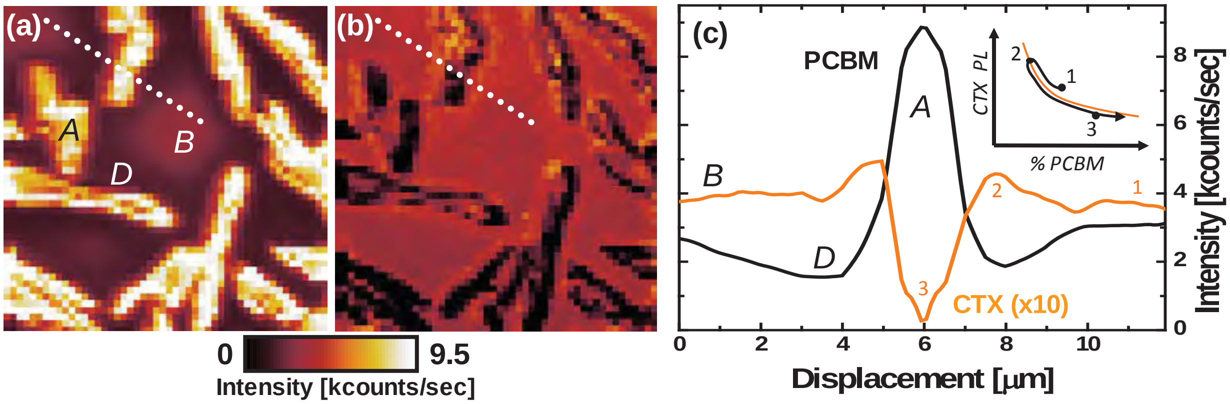

FIG. 1: Confocal photoluminescence (PL) images of phase separation in a thermally annealed polymer:fullerene film depicting (a) fullerene (PCBM) and (b) charge transfer exciton (CTX) emission. The *A*, *D*, and *B* notations represent the agglomerate, depletion, and blend zones, respectively. (c) Profiles of the PCBM and CTX emission along the line shown in (a and b). Panel (c) inset demonstrates the behavior of CTX emission as a function of PCBM loading, as represented by points (1, 2, 3) in the CTX line profile.

Plasma-phase synthesis of vertically-aligned metal oxide nanowires for gas sensing and light harvesting applications

Travis Koh, Evan C. O'Hara, and Michael J. Gordon

Department of Chemical Engineering, University of California, Santa Barbara

One-dimensional metal oxide and semiconductor nanostructures (i.e., nanowires, NWs) have the potential to play a pivotal role in many future technologies related to energy conversion, catalysis, and microelectronics. For example, semiconductor NWs have been used as photo- and electro-catalysts, light emitters, transistors, and microelectronic interconnects, as well as light harvesters and scatterers in solar cell applications. Metal oxide NWs have also been used as building blocks to create novel catalytic materials, chemical sensors, and optoelectronic devices.

The first part of the talk will detail a novel, plasma-phase synthesis technique developed in our lab (supersonic plasma microjets) for the growth of semiconducting metal oxide NWs to drive the anisotropic growth of CuO, PdO, NiO, SnO_2 and α-Fe_2O_3 nanostructures. Briefly, NW growth is initiated using the high pressure microplasma jet to deposit a thin metal oxide layer (~20 nm), which subsequently provides nucleation centers for the vertical growth of one-dimensional NWs. Both seeding and NW growth are achieved in a single step using volatile organometallic CVD precursors as active metal sources. Through careful control of the precursor flux, plasma current, background gas atmosphere, and substrate temperature, nucleation centers can be seeded at different times in the deposition process, resulting in the growth of aligned nanowires or, fractal-like "nano-trees". The second part of the talk will highlight potential applications of the microplasma-deposited films, namely, semiconducting CuO/SnO_2 NWs and nano-trees for light harvesting in ruthenium-based dye-sensitized solar cells and gas detection using SnO_2 NW arrays.

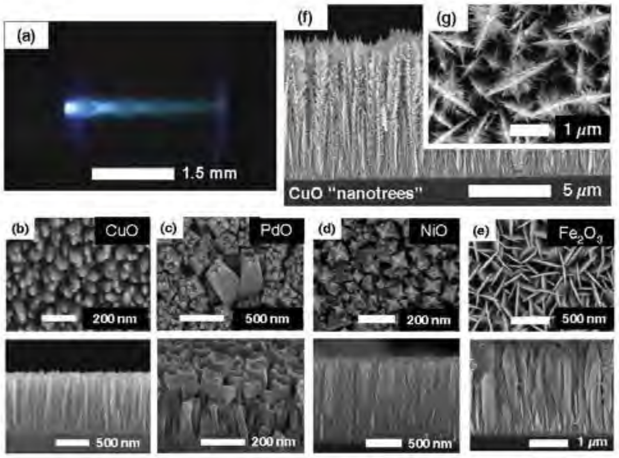

Figure 1: (a) Plasma microjet in operation. (b-e) CuO, PdO and NiO NWs, α-Fe_2O_3 nano-blades. (f-g) CuO nano-trees.

Functionalized mesoporous silica and carbon materials for fuel cell applications

Donghun Kim

Department of Chemical Engineering, University of California, Santa Barbara, California

Mesoporous materials synthesized by using self-assembly of polymer surfactants provide well-ordered pore structures and large uniform pore sizes (>2 nm) that enhance intra-pore mass transports and increase intra-pore-surface functional moieties. Diverse compositions of mesoporous inorganic-organic materials in addition to surface functionalization can provide a broad range of properties, which can provide new materials for important electrochemical applications that are currently limited by conventional materials. Two different functionalized mesoporous materials for fuel cell applications will be presented: (1) proton exchange membranes for operation of hydrogen fuel cells at elevated temperatures and (2) non-precious metal catalysts for oxygen reduction reactions, which are suggested by Department of Energy as requiring crucial breakthroughs to implement wide use of hydrogen fuel cells.

Acid-functionalized mesoporous aluminosilica membranes have been developed for elevated temperature(> 100 °C) operation of hydrogen fuel cells. Operation at elevated temperature provides several benefits, such as faster reaction kinetics, higher permissible CO levels in the hydrogen fuel feed, easier water management, and more useful heat recovery. However, conventional polymeric membrane materials membranes (e.g., perfluorosulfonic acid ionomers, Nafion®) have been generally limited by their low proton conductivities under such conditions, due to their poor water retention properties, which cause their “soft” hydrophilic proton-conducting channels to become discontinuous. By comparison, the robust channels of mesoporous silica membranes are maintained even at high temperatures and low humidity conditions. In addition, the relatively large pore sizes and volumes of mesoporous silica materials provide opportunities to incorporate diverse functional moieties onto the internal pore surfaces or within the siliceous framework. By incorporating thermally stable organic moieties, hydrophilic aluminosilica, and acidic moieties into the mesoporous silica membranes, good mechanical properties, high water retention, and high ion mobilities are achieved that yield high proton conductivities at temperatures of ca. 120-150 °C and low humidity conditions in operating fuel cells.

Using a similar functionalization approach, mesoporous silica materials can be converted into mesoporous carbon materials that overcome several cost and performance limitations associated with electrode or electrocatalyst properties of fuel cells. Highly graphitic mesoporous carbon materials exhibit a combination of high electrical conductivities, high surface areas, good thermal and chemical stabilities, and improved mass transport properties, compared to conventional carbon materials. In addition, mesoporous carbon materials can be functionalized with earth-abundant Fe and nitrogenous surface species to obtain cost-effective oxygen reduction activities that may replace expensive precious-metal catalysts (typically Pt) in fuel cell cathodes. Resultant Fe,N-functionalized mesoporous carbon catalysts show good oxygen reduction activities that are comparable to but slightly lower than Pt catalysts in acid electrolytes and are higher in alkaline electrolytes. Prospects will be discussed for integrating both the hybrid proton-exchange membranes and the non-precious-metal electrocatalysts into commercial fuel cells and devices.

Water-assisted mechanisms reconcile experimental and calculated kinetics and thermodynamics for the sequential complexation of CH_3ReO_3 by H_2O_2

Taeho Hwang [(a)], Bryan R. Goldsmith[(a)], Baron Peters [(a,b)], and Susannah L. Scott [(a,b)]

(a) Department of Chemical Engineering, University of California, Santa Barbara, CA 93106
(b) Department of Chemistry and Biochemistry, University of California, Santa Barbara, CA 93106

A combined computational and experimental study of the reaction of CH_3ReO_3 (methyltrioxorhenium, MTO) with H_2O_2 was undertaken to understand the origins of large discrepancies in the previously reported experimental reaction kinetics, as well as between computed and experimentally measured thermodynamics. The sequential transformation of MTO to a monoperoxo complex $CH_3ReO_2(\eta^2\text{-}O_2)$, **A**, and a diperoxo complex $CH_3ReO_2(\eta^2\text{-}O_2)_2(H_2O)$, **B**, was studied experimentally in aqueous CH_3CN (containing 2.0 M H_2O). The reaction displays biexponential kinetics, with activation parameters $\Delta H^\ddagger$ and $\Delta S^\ddagger$ of 8.4 kJ mol^{-1} and -223 J K^{-1} mol^{-1}, respectively, for the formation of **A**, and 20.7 kJ mol^{-1} and -247 J K^{-1} mol^{-1} for its hydrolysis. The corresponding values $\Delta H^\ddagger$ and $\Delta S^\ddagger$ for the formation of **B** are 20.0 kJ mol^{-1} and -206 J K^{-1} mol^{-1}, respectively, while for hydrolysis of **B**, they are 63.1 kJ mol^{-1} and -104 J K^{-1} mol^{-1}. Whereas previous computational studies were inconsistent with reported thermodynamics for these reactions, we show that a water-assisted mechanism brings the thermodynamics and kinetics into closer agreement.

References:
[1] Wang, W. D.; Espenson, J. H. *Inorganic Chemistry* **1997**, *36*, 5069-5075.
[2] Abu Omar, M. M.; Hansen, P. J.; Espenson, J. H. *J. Am. Chem. Soc.* **1996**, *118*, 4966-4974.